

# Characterizing the Surface Energy Budget Relationship to Hypoxia of Western Long Island Sound in mid-Summer 2004 and 2005

Steven R. Schmidt<sup>†</sup> and James P. Boyle Ph.D.

*Physics, Astronomy, and Meteorology Department, Western Connecticut State University, Danbury, Connecticut*

## ABSTRACT

During the summer months, a hypoxic condition (a lack of oxygen) develops in the bottom waters of Western Long Island Sound (WLIS). This is primarily caused by excessive amounts of nitrogen being discharged into the Sound and by the natural stratification of its waters. This stratification inhibits atmospheric oxygen from penetrating into the bottom waters of the Sound. Though excessive amounts of nutrients are accredited with the development of this hypoxic condition, they may not completely explain why certain years are more severe than others. Using measured and modeled meteorological and radiation data (i.e. air temperature, water temperature, global irradiance, etc.) the surface energy budget for WLIS is characterized for the period from 17 July [Julian Day (JD) 198] to 05 Aug. (JD 217) in both 2004 and 2005. From this characterization there is a better understanding of how the variation in net surface heat transfer between years may impact the severity of hypoxia. Our results suggest a greater net energy input occurred in 2005 correlating with more severe hypoxic conditions.

(Revision 'L' Finalized April 28<sup>th</sup>, 2010)

**HYPOXIA SEVERITY.** The period between 17 July and 5 Aug. was chosen for analysis because of the extreme contrast observed between the 2004 and 2005 hypoxia severity in the first week of August. Figure 1 shows maps from the Connecticut Department of Environmental Protection (CTDEP) depicting the severity of hypoxia. A comparison of these maps indicates the first week of August 2005 is far more severe than August 2004.

**DATA SPECIFICS.** Data was collected and used from the National Data Buoy Center (NDBC) and the National Solar Radiation Database (NSRDB).

Meteorological data for this analysis is from the moored buoy ID 44040 (aka the WLIS mooring). The following variables are used:

- Air Temperature (3 m height)
- Water Temperature (1 m depth)
- Dew-point Temperature (3 m height)
- Barometric Pressure (surface)
- Wind Speed & Direction (3.5 m height)

A linear interpolation method is used to fill periods of missing data.

The NSRDB uses meteorological data from ASOS (Automated Surface Observation System) stations to infer downwelling solar radiation. For this analysis, NSRDB modeled solar radiation data is used from the following stations:

- LaGuardia Airport, New York - Station ID 725030
- Republic, New York - Station ID 744864
- Westchester Airport, New York - Station ID 725037

NSRDB data is available for several models. The State University of New York (SUNY) model data is used in this analysis as follows:

- YYYY-MM-DD – Year / Month / Day
- HH:MM (LST) – Hour / Minute (Local Standard Time)
- SUNY Glo ( $W m^{-2}$ ) – Global Solar Radiation
- SUNY Dir ( $W m^{-2}$ ) – Direct Solar Radiation

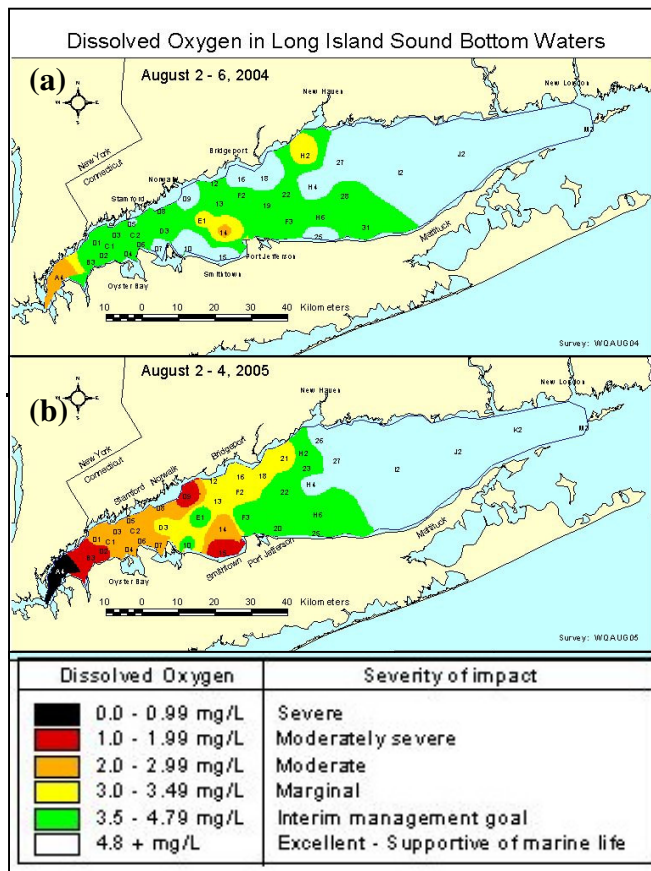


**FIGURE 1 – Hypoxia Severity:** Hypoxia severity as depicted by the CTDEP in color contours for 2004 (figure 1a) and 2005 (figure 1b).

<sup>†</sup>Corresponding author address: Steven R. Schmidt, Physics & Meteorology Dept. Western Connecticut State University, 181 White Street, Danbury, CT 06810, [schmidt067@connect.wcsu.edu](mailto:schmidt067@connect.wcsu.edu)

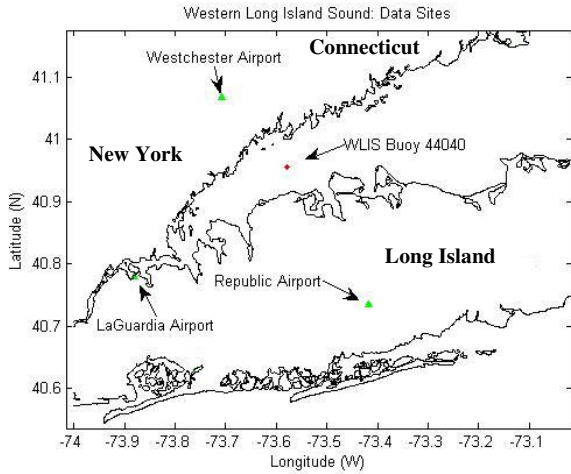


**FIGURE 2 – Data Sites:** Location of sites for data analysis. Green triangles are representative of land-based stations. Red diamonds represent buoy locations.

**TEMPERATURE ANALYSIS.** WLIS buoy and land based data are first analyzed to detect differences in meteorological and oceanic measurements between years. Of considerable initial interest are near surface air and water temperature as both are a measure of the amount of internal energy present and are related to heat transfer. Furthermore, the solubility of dissolved oxygen depends on water temperature.

Air Temperature: Figure 3 is a scatter plot year-to-year comparison of air temperature for the WLIS buoy. Air temperature was higher in 2005 (the more severe hypoxic year) with approximately 82% of all plots above the 1:1 slope reference line in the figure.

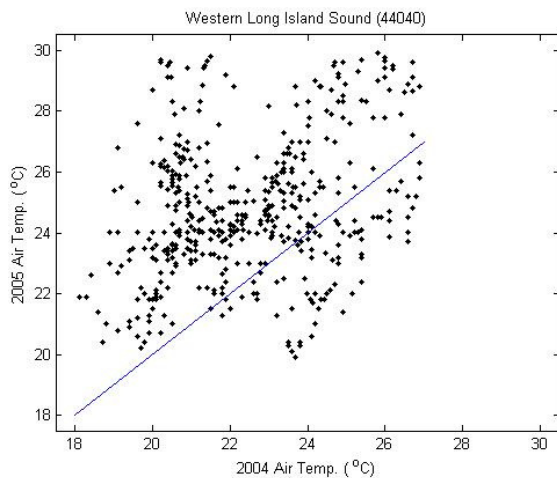


**FIGURE 3 - Air Temperature:** Scatter plot of 2004 vs. 2005 air temperatures for the western LIS buoy. Blue reference line has a slope of 1:1.

Water Temperature: Comparison of water temperature (Figure 4) indicates higher values in 2005 for 99 % of the time during this three-week period under investigation.

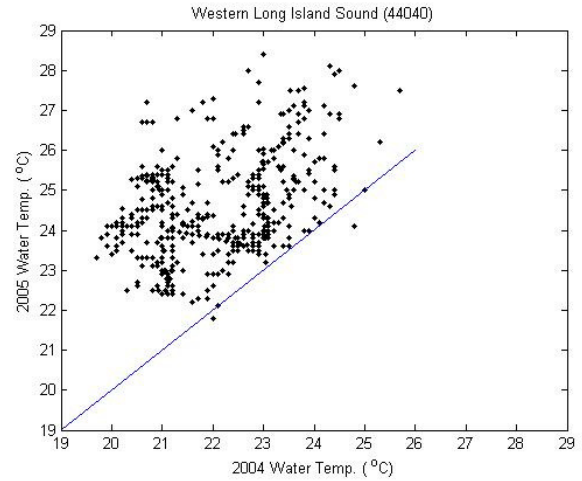


**FIGURE 4 - Water Temperature:** Scatter plot of 2004 vs. 2005 water temperatures for the western LIS buoy. Blue reference line has a slope of 1:1.

Conclusions for Near Surface Temperature: Tables I & II provide statistical values for air temperature in both years. Minimum, maximum, mean, and median temperatures were all higher during 2005.

**Table I: Air Temperature Statistics**

Year	Minimum	Maximum	Mean	Median
2004	18.1 °C	26.9 °C	22.5 °C	22.5 °C
2005	19.9 °C	29.9 °C	24.8 °C	24.5 °C

**Table II: Water Temperature Statistics**

Year	Minimum	Maximum	Mean	Median
2004	19.7 °C	25.7 °C	22.1 °C	22.1 °C
2005	21.8 °C	28.4 °C	24.5 °C	24.3 °C

**ENERGY FLOW.** There are several mechanisms through which energy can enter or leave the water column. Energy flow downward into LIS is defined as negative; whereas energy transport from LIS to the atmosphere is defined as positive. In order to develop a reasonable understanding of the water energy budget, the following mechanisms of energy transfer at the air-water interface are considered:

*1 – Net global solar irradiance:* Net global solar irradiance ( $SWR_{NET}$ ) is the sum of direct and diffuse solar radiation which penetrate into the water column – input of energy to the water. Direct solar radiation ( $SWR_{dir}$ ) is un-scattered solar radiation that reaches the surface. Diffuse solar radiation ( $SWR_{diff}$ ) is solar radiation that after having been scattered by hydrometeors, atmospheric gases and/or aerosols reaches the surface. Equation (1) shows how  $SWR_{NET}$  is determined from both direct and diffuse radiation assuming a constant water surface albedo ( $\alpha$ ) of 5.5 %. The data for the direct and diffuse solar radiation components are available from the SUNY solar radiation model.

$$SWR_{NET} = (1-\alpha) (SWR_{dir} + SWR_{diff}) \quad (W m^{-2}) \quad (1)$$

2 – *Net Infrared (Longwave) Radiation*: Net infrared radiation is the sum of Incoming and Outgoing Longwave Radiation (LWR). Incoming (downwelling) Infrared Radiation ( $LWR_{\text{down}}$ ) is the amount of infrared radiation emitted from the atmosphere and clouds that reaches the surface – input of energy to the water. Outgoing (upwelling) Infrared Radiation ( $LWR_{\text{up}}$ ) is the amount of infrared radiation emitted from the water’s surface due to its temperature – output of energy from the water. Net infrared radiation is determined through use of equation (2) where a constant water surface longwave radiation emissivity ( $\epsilon$ ) of 0.97 is assumed.

$$LWR_{\text{NET}} = \epsilon (LWR_{\text{down}} + LWR_{\text{up}}) \quad (\text{W m}^{-2}) \quad (2)$$

3- *Sensible Heat Flux*: Sensible heat flux (SHF) is energy transfer due solely to a temperature difference between the atmosphere and the WLIS water – either energy input or output ( $\text{W m}^{-2}$ ).

4- *Latent Heat Flux*: Latent heat flux (LHF) is energy transfer due to a change in phase of a substance (i.e. evaporation of liquid water into water vapor) – generally an energy output from the water ( $\text{W m}^{-2}$ ).

By summing these four components the net heat transfer is determined for a specific time or given period per equation (3).

$$\text{Net Surface Heat Flux} = SWR_{\text{NET}} + LWR_{\text{NET}} + SHF + LHF \quad (3)$$

**GLOBAL IRRADIANCE.** NSRDB modeled radiation data for LaGuardia, Westchester, and Republic airports is averaged to obtain values for the WLIS buoy location. From this averaging, estimates of direct beam ( $SWR_{\text{dir}}$ ) and global irradiance ( $SWR_{\text{NET}}$ ) over WLIS are obtained. Figure 5 compares results for 2004 against 2005 for the global irradiance of the WLIS buoy prior to the application of a 5.5% albedo.

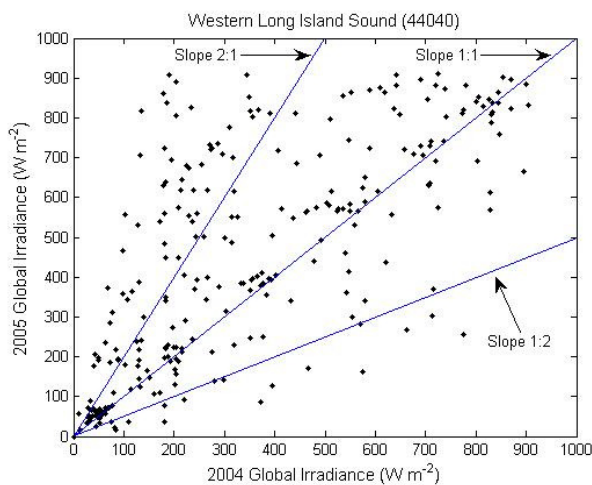


**FIGURE 5 – Global Irradiance:** Scatter plot of 2004 vs. 2005 Global Irradiance for the western LIS buoy.

Considering the distribution of the data with respect to the reference lines provided, a greater input of solar radiation occurs in 2005. The three-week integration of net global irradiance ( $SWR_{\text{NET}}$ ) for 2005 is  $-112,420 \text{ W m}^{-2}$ , approximately 25% larger than the 2004 net input of  $-87,317 \text{ W m}^{-2}$ .

**NET INFRARED RADIATION.** Net longwave radiation (LWR) consists of downwelling and upwelling components, both of these are determined.

Downwelling Longwave Radiation: Atmospheric gases, aerosols, and hydrometeors (cloud water droplets, cloud ice crystals and precipitation) emit infrared radiation in all directions, including toward the surface. As a result, the amount of cloud cover and cloud base temperature influence the amount of downwelling longwave radiation. As cloud fraction increases, so does downwelling infrared. Estimates of  $LWR_{\text{down}}$  are made using the bulk model *Prata (1996) for clear sky as modified for cloud forcing by Diak (2000)*.

To determine cloud fraction, the derived values for direct beam radiation are divided by theoretical ‘clear-sky’ expected values and subtracted from unity. Negative solar elevation angle values are omitted and values greater than one are renormalized. This method only allows estimation of cloud fraction values for daylight hours. Nighttime cloud fraction values are linearly interpolated between the sunset and the sunrise values.

In summary,  $LWR_{\text{down}}$  is derived using the estimated cloud fraction and the NDBC WLIS buoy meteorological data applied to the Prata (1996) and Diak (2000) parameterizations.

Upwelling Infrared:  $LWR_{\text{up}}$  is calculated using the Stefan-Boltzmann Law and water temperature as follows:

$$LWR_{\text{up}} = \sigma_{\text{sb}} T_{\text{sfc}}^4 \quad (4)$$

Conclusion for Net Longwave Radiation: In 2005, the net infrared radiation energy loss is  $16,746 \text{ W m}^{-2}$ , approximately 348% more than the value for 2004:  $12,155 \text{ W m}^{-2}$ . Water surface temperature was greater in 2005 than in 2004 resulting in a 3 % greater  $LWR_{\text{up}}$ ; therefore, the greater net LWR energy loss suggests fewer clouds during 2005; fewer clouds would have reduced the amount of atmospheric radiation emitted towards the surface ( $LWR_{\text{down}}$ ), thus increasing the amount of energy loss.

**LATENT & SENSIBLE HEAT FLUXES.** Latent & sensible heat fluxes are estimated using the Coupled Ocean-Atmosphere Response Experiment (COARE) algorithm 3.0 (Fairall, 1998, 2003). This parameterization requires input of: estimated downwelling infrared and global radiation as well as WLIS buoy meteorological data.

Figure 6a shows a year-to-year comparison of time series’ for estimated latent heat fluxes. Latent heat fluxes were greater during 2005 with a net energy loss of  $21,627 \text{ W m}^{-2}$  (approximately 153 % greater than the 2004 value of

8,567  $\text{W m}^{-2}$ ). Such a difference is partially a result of greater wind speed in 2005 for 59% of the analysis period.

Figure 6b is a time series comparison of 2004 (black) and 2005 (red) sensible heat fluxes. Both outgoing and incoming sensible heat fluxes are generally greater in 2005, a result of both greater air/water temperature difference and greater wind speed. The net sensible heat flux calculated for 2004 is  $-395 \text{ W m}^{-2}$  (incoming) while 2005 is 83 % larger with a value of  $-722 \text{ W m}^{-2}$  (incoming).

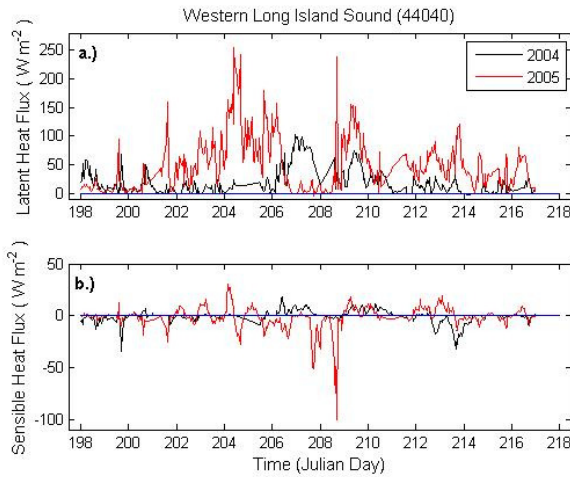


**FIGURE 6a – Latent Heat Flux:** Time series plot comparison of latent heat flux for 2004 (black) and 2005 (red).

**FIGURE 6b – Sensible Heat Flux:** Time series plot comparison of sensible heat flux for 2004 (black) and 2005 (red).

### ANALYSIS OF NET SURFACE HEAT TRANSFER.

Figures 7 & 8 both indicate, as expected, that the greatest source of thermal energy input for both years is global solar irradiance (blue). Other heat flux components, such as sensible heat and net infrared fluxes are significantly smaller.

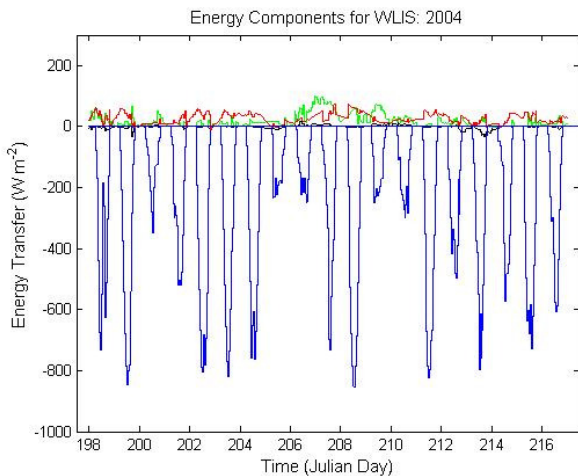


**FIGURE 7 - 2004 Energy Components:** Individual energy components from July 16<sup>th</sup> to August 4<sup>th</sup>, 2004. Depicted is Global Irradiance (blue), Net Infrared (red), Latent Heat Flux (green), Sensible Heat Flux (black).

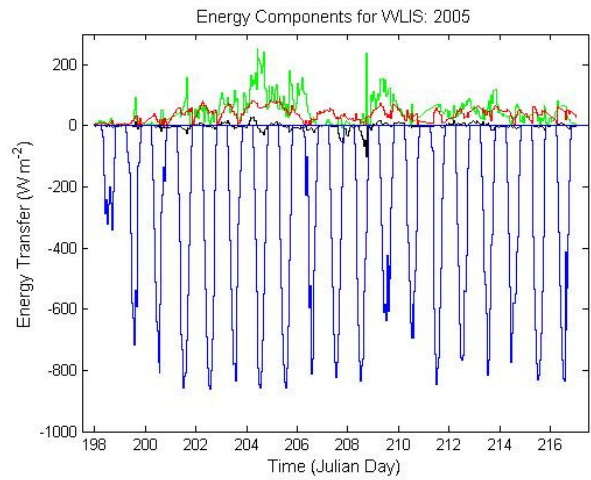


**FIGURE 8 - 2005 Energy Components:** Individual energy components from July 17<sup>th</sup> to August 5<sup>th</sup>, 2004. Depicted is Global Irradiance (blue), Net Infrared (red), Latent Heat Flux (green), Sensible Heat Flux (black).

Comparison of these figures suggests that 2004 has fewer clear sky days than 2005 – this is the a critically important difference between years. The biggest energy sinks for both years are latent heat and net infrared fluxes. Net latent heat flux in 2005 is greater than any net energy sink in both years. Overall, WLIS had a larger net gain of thermal energy in 2005. Table III shows the net heat input for both years – net heat input was 11.5 % greater in 2005.

**Table III: Energy Transfer Mechanism Totals**

Transfer Mechanism	2004 ( $\text{W m}^{-2}$ )	2005 ( $\text{W m}^{-2}$ )
Global Irradiance	-87,317	-112,420
Sensible Heat Flux	-395	-722
Latent Heat Flux	8,567	21,672
Net Infrared	12,155	16,746
Net Heat Input	-66,991	-74,724

**CONCLUSION.** A correlation between hypoxia severity and water surface heat flux is suggested as a result of this research. Evaluation of estimated global irradiance, latent heat flux and net infrared for the 2004 and 2005 three-week data sets seem to indicate that more cloud cover is present for the less severe hypoxic year of 2004. Greater cloud cover results in a decreased amount of  $\text{SWR}_{\text{NET}}$  reaching the surface as well as a reduced amount of energy loss due to  $\text{LWR}_{\text{up}}$  as is shown to exist.

Lower  $\text{SWR}_{\text{NET}}$  input during 2004 may be critically important for a less severe hypoxic condition in the first week of August. During the three-week period analyzed other components of energy transfer (namely latent and outgoing longwave) were indicative of significantly greater losses in the more severe hypoxic year of 2005. Thus, the resulting difference in net heat energy input appears to be primarily due to lower  $\text{SWR}_{\text{NET}}$  in 2004.

**FUTURE WORK.** This research provides a quantitative analysis of the net water surface heat flux for a three-week period in 2004 and 2005. There is potential for additional analysis. Rain heat flux (the sensible heat flux due to input of rain water) is not considered in this analysis and has been found to be a significant component of net surface heat – accounting for 15%-60% of the net heat flux for any single rain event (S. P. Anderson et al. 1998). It is, for this reason, desirable to perform an analysis that considers rain heat flux and particularly its influence on buoyancy, salinity, and dissolved oxygen levels.

Characterization of the mixed layer in WLIS region through use of the Price-Weller-Pinkel (PWP) mixed layer model (J. F. Price et al. 1986) is also recommended. Characterizing the mixed layer strength and depth would support determination of the impact of surface heat flux on the static stability of the surface and mixed layers of WLIS and its influence on the severity of hypoxia.

**ACKNOWLEDGEMENTS.** This research could never have been done without the support of Vincent Breslin Ph. D, professor of Science Education and Environmental Sciences at Southern Connecticut State University. Also, many thanks to the University of Connecticut's Marine Sciences for the operation of WLIS buoy's 44040 & 44039 and to Kay Howard-Stroebel for providing some of this data.

#### **REFERENCES.**

- Anderson, S. P., A. Hinton, R. A. Weller, 1998: Moored Observations of Precipitation Temperature. *J. Atmos. & Oceanic Tech.*, 979-986.
- Arya, S. Pal. *Introduction to Micrometeorology*. San Diego, Calif. [u.a.]: Acad., 2008. Print.
- Diak, G. R., W. L. Bland, J. R. Mecillalski, M. C. Anderson, 2000: Satellite-Based estimates of longwave radiation for agricultural application. *Agricultural & Forest Meteorology*. V. 103, 349-355.
- Fairall, C. W., E. F. Bradley, D. P. Rogers, J. B. Edson, and G. S. Young, 1996a: Bulk Parameterization of air-sea fluxes in TOGA COARE. *J. Geophys. Res.*, **101**, 3747-3767.
- Fairall, C. W., E. F. Bradley, J. E. Hare, A. A. Grachev, J. B. Edson, 2003: Bulk Parameterization of Air-Sea Fluxes: Updates and verification for the COARE Algorithm. *J. Clim.*, 571-591.
- Flament, P., M. Sawyer, 1995: Observations of the Effect of Rain Temperature on the Surface Heat Flux in the Intertropical Convergence Zone. *J. P. Ocean.*, 413-419.
- Garratt, J. R., A. J. Prata, 1996: Downwelling Longwave Fluxes at Continental Surfaces – A Comparison of Observations with GCM Simulations and Implications for the Global Land-Surface Radiation Budget. *J. Clim.*, 646-555.
- Prata, A. J., 1996: A long-wave formula for estimating downward clear-sky radiation at the surface. *Quart. J. Roy. Meteor. Soc.*, 122, 1127-1151.
- Price, J. F., R. A. Weller, and R. Pinkel, 1986; Diurnal cycling: Observations and models of the upper ocean

response to diurnal heating, cooling, and wind mixing. *J. Geophys. Res.*, 91, 8411-8427.

Stull, Roland B., and C. Donald. Ahrens. *Meteorology for Scientists and Engineers*. Pacific Grove, CA: Brooks/Cole, 2000. Print.